

SYNTHESIS AND CHARACTERIZATION OF ZEOLITE/Fe₃O₄ NANOCOMPOSITE BY GREEN QUICK PRECIPITATION METHOD

HOSSEIN JAHANGIRIAN^{a,b,*}, MOHD HALIM SHAH ISMAIL^{a,*}, MD JELAS HARON^c, ROSHANAK RAFIEE-MOGHADDAM^{b,d}, KAMYAR SHAMELI^e, SORAYA HOSSEINI^a, KATAYOON KALANTARI^e, ROSHANAK KHANDANLOU^e, ELHAM GHARIBSHAHI^f, SEPIDEH SOLTANINEJAD^f

^a*Department of Chemical and environmental engineering, Faculty of engineering, Universiti Putra Malaysia, 43400 UPM, Serdang, Selangor, Malaysia*

^b*R & D Section of ZargolChemi Productive Co., ZCPC, (3188113984) Eshtehard Industrial Park, Alborz, Iran*

^c*Chemistry Unit, Centre of Foundation Studies for Agricultural Science, Universiti Putra Malaysia, 43400 UPM Serdang, Selangor, Malaysia*

^d*School of Chemical Sciences and Food Technology, Faculty of Science and Technology, Universiti Kebangsaan Malaysia, 43600 UKM Bangi, Selangor, Malaysia*

^e*Department of Chemistry, Faculty of Science, Universiti Putra Malaysia, Serdang 43400 UPM, Selangor, Malaysia*

^f*Department of Physics, Faculty of Science, Universiti Putra Malaysia, Serdang 43400 UPM, Selangor, Malaysia*

A green quick precipitation method was successfully used for synthesis of magnetic iron oxide nanoparticles (Fe₃O₄-NPs) on the surface of sodium/potassium type zeolite. Ferric chloride, ferrous chloride and sodium hydroxide aqueous solutions were used in the synthesis and coating of the Fe₃O₄-NPs on the surface of the zeolite to produce the zeolite/magnetic iron oxide nanocomposite (zeolite/Fe₃O₄ -NCs). The reaction was performed in aqueous suspension phase under the ambient condition as green chemistry method. Characterization with Fourier transforms infrared spectroscopy (FT-IR), powder X-ray diffraction (PXRD), scanning electron microscopy (SEM), energy dispersive X-ray fluorescence (EDXF) and transmission electron microscopy (TEM) confirmed the formation of Fe₃O₄-NPs with mean particle sizes of 3.55±1.02 nm on the surface of the zeolite.

(Received June 19, 2013; Accepted October 15, 2013)

Keywords: Nanocomposites; Zeolite, Iron oxide nanoparticles, X-ray powder diffraction, Transmission electron microscopy, Scanning electron microscopy, Energy dispersive X-ray fluorescence

1. Introduction

In the recent years, nanocomposite materials constitute a rapidly evolving field of science and technology due to various interesting properties and subsequently different applications. They have been widely applied in biotechnology and new chemistry sciences such as: using in toxicology [1], preparation of electrochemical sensor [2], immunosensor for pesticides detection [3], use of magnetic nanowires as sensors for electric or nonelectric quantities [4], sensor for sensitivity of nitrogen dioxide [5], membrane for alkaline fuel cells [6], silver-polymer composite materials with antibacterial property [7], ceramic-polymer composites doped with gold nanoparticles for medical and dentistry applications [8], catalyst [9] and fire retardant compounds

* Corresponding author: kamran.jahangirian@gmail.com

preparation [10]. Iron and its compounds had been important in human life due to its biological and chemical properties. Iron oxides are widespread in earth cortex and play an important role in nature. Recently they have widely utilized in nanocomposite for various application [11-14]. Zeolites are microporous, aluminosilicate compounds which are as natural minerals or synthesized. They were widely used in industry for water and waste water treatment, waste gas treatment, as catalysts, as molecular sieve, in the production of laundry detergents, nuclear processing medicine and in agriculture purposes for the preparation of advanced materials and recently to produce the nanocomposites [15-19].

Previously, investigators have performed various synthesis methods for producing of Fe_3O_4 -NPs. Pinna et. al. prepared nanocrystalline magnetite in a simple one-pot reaction process by nonaqueous route method [20], they dissolved iron(III) acetylacetone in benzyl alcohol and treated in an autoclave between 175 and 200 °C and prepared monocrystalline magnetite particles with sizes ranging from 12 to 25 nm. Chiu et. al. used pyrolysis method to prepare high quality colloidal Fe_3O_4 nanocrystals within the range of 4–18 nm diameter [21]. Their method was based on the pyrolysis of self-made iron oleate precursor by using oleic acid which was extracted from natural palm-oil as capping ligands. Tang et. al. applied a sol–gel method to prepare nanostructured magnetite (Fe_3O_4) thin films at 300°C [22]. They used N, N-dimethyl formamide as drying control agent and obtained magnetite thin film with root mean square roughness of only 2 nm and nanograins of narrow size distribution with the average diameter of 12.5 nm. Vijaya et. al. used ultrasound radiation for dispersing amorphous magnetite in polyvinyl alcohol and obtained magnetite nanoparticles of 12–20 nm in diameter [23]. Martinez-Mera et. al. synthesized iron oxide nanoparticles in the range of 4–43 nm using a colloidal method at room temperature, without the use of surfactants but using precursors like $\text{FeCl}_3 \cdot 6\text{H}_2\text{O}$ and $\text{FeCl}_2 \cdot 4\text{H}_2\text{O}$ in deionized water free of dissolved oxygen and ammonia solution [24]. Many of the above methods generally use of hazardous solvents and raw materials with some of them use high energy which are not environmental friendly.

In this work, we synthesized Fe_3O_4 -NPs on the surface of zeolite as coated nano thin layer and produced zeolite/ Fe_3O_4 -NCs directly by quick precipitation method in just one step reaction. The reaction was performed under mild conditions, using low energy, low cost raw materials and under friendly environment (due to using of non-hazardous solvent and raw materials and inert residue) which indicate the method is based on green chemistry. This is the most important advantage of current method.

2. Experimental

2.1. Materials

$\text{FeCl}_3 \cdot 6\text{H}_2\text{O}$ and $\text{FeCl}_2 \cdot 4\text{H}_2\text{O}$ were supplied by Merck, Germany, Zeolite (96096, Potassium, 3A° type) was purchased from Sigma-Aldrich, USA, HCl, NaOH, were obtained from Systerm Co., Malaysia.

2.2. Synthesis of zeolite/ Fe_3O_4 -NCs

For the synthesis of zeolite/ Fe_3O_4 -NCs, first 4.0 g of zeolite was added to 40 mL of distilled water and slowly stir for 10 min. until homogenate suspension was obtained. After that a desired quantity of FeCl_3 and FeCl_2 solutions with molar ratio of 2:1 was added into the suspension and stir for 30 min. Then while the mixture was being stirred vigorously about 20 mL of 2.5 M NaOH solution was slowly added and vigorous stirring was continued for another 30 min. The synthesized product (zeolite/ Fe_3O_4 -NCs) was then filtered, washed with distilled water and finally air dried at room temperature or dried in oven at 50°C. All the experiments were performed at ambient temperature and pressure.

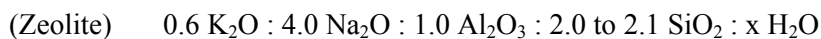
2.3. Characterization Methods and Instruments

Fourier transform infrared (FT-IR) spectroscopy was used to study the structures of the zeolite and zeolite/Fe₃O₄-NCs. The FT-IR spectra were recorded in the range of 400–4,000 cm⁻¹ and 100–700 cm⁻¹ utilizing a Perkin Elmer GX - FT-IR spectrophotometer. The powder X-ray diffraction (PXRD) with Cu K α radiation was used to measure the crystallinity of samples. Transmission electron microscopy (TEM) was applied to measure the morphology and particle size of the synthesized products. For this purpose a drop of suspended product in distilled water was dripped onto a covered copper grid then the TEM observations were carried out using a Hitachi H-7100 electron microscope and after that the particle size distributions were estimated by the UTHSCSA Image Tool software, version 3.00. Scanning electron microscopy (SEM) was applied to observe morphology of zeolite and zeolite/Fe₃O₄-NCs. The SEM with Energy dispersive X-ray fluorescence (EDXF) spectroscopy was performed utilizing a JEOL, JSM-7600F instrument.

3. Results and Discussion

3.1. Synthesis of zeolite/Fe₃O₄-NCs

The following formulation of zeolite which used in this investigation (96096, Potassium, 3A° type) shows the molecule is made up of silicon, aluminium, sodium and potassium oxides and its pore diameter is about 3A°.



In the first step, when FeCl₃ and FeCl₂ solutions are mixed with the zeolite, sodium and potassium ions are exchanged by iron(II) and iron(III) ions. In the next step, Fe₃O₄ precipitates on the surface (external surface and internal surface of pores) of zeolite when the NaOH solution is added to the reaction mixture. The simplified chemical equation of zeolite/Fe₃O₄-NCs synthesis is shown in Figure 1. The powdered particles of the product (zeolite/Fe₃O₄-NCs) was found very easily attracted to magnet indicating that the product has magnetic property and the synthesis has been successful.

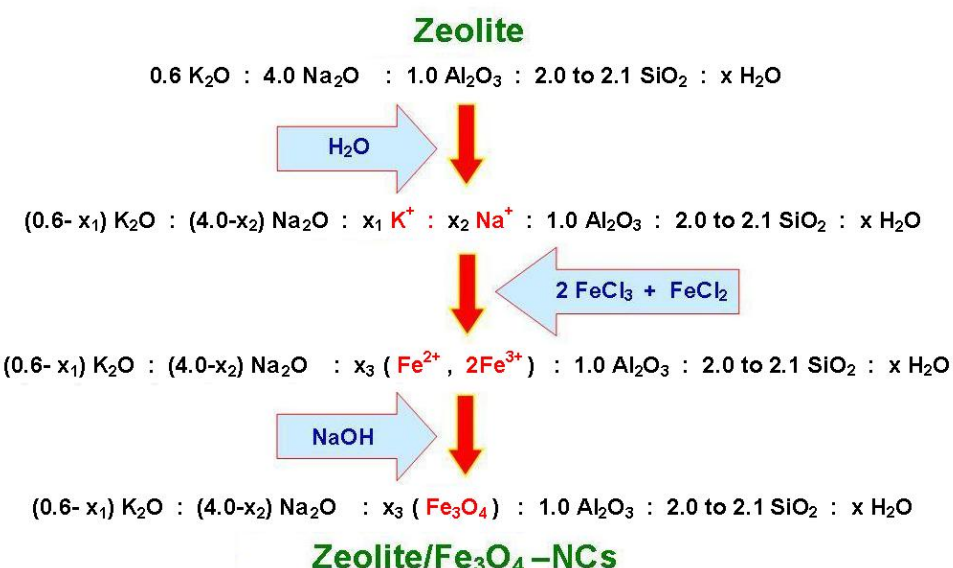


Fig. 1. The simplified chemical equation of zeolite/Fe₃O₄-NCs synthesis.

$$[x_3 = (x_1 + x_2) / 4]$$

3.2. FT-IR spectroscopy

3.2.1. Near FT-IR spectroscopy

The near FT-IR spectra of zeolite (a) and zeolite/Fe₃O₄-NCs (b) are shown Figure 2. The zeolite spectra (a) in Figure 2 shows an absorption in the region of 3627 cm⁻¹ corresponds to terminal silanol groups on the external surface of the zeolite crystals [25,26]. This peak overlapped with wide and strong peaks correspond to O-H stretching in the spectral regions 3100 to 3500 cm⁻¹. The peak in the region of 1673 cm⁻¹ corresponds to O-H bending vibration. The absorption appeared in the regions of 900 to 1200 cm⁻¹ are resulted from stretching and bending modes of Si-O or Al-O in zeolite framework for example the bands around 1120 cm⁻¹ are assigned to the asymmetric and symmetric stretching modes of internal tetrahedra, and the bands around 1017 cm⁻¹ are associated with the asymmetric and symmetric stretching modes of external linkages [25-27]. Figure 2 also shows that zeolite/Fe₃O₄-NCs spectra (b) does not significantly different from the zeolite spectra (a) in the spectral regions 700 to 4000 cm⁻¹. This fact indicates that zeolite structure has not changed in this reaction. The variations of zeolite/Fe₃O₄-NCs spectra (b) compared to the zeolite spectra (a) in the far FT-IR spectral regions of 700 to 300 cm⁻¹ correspond to the Fe₃O₄-NPs will be described in detail in the next section.

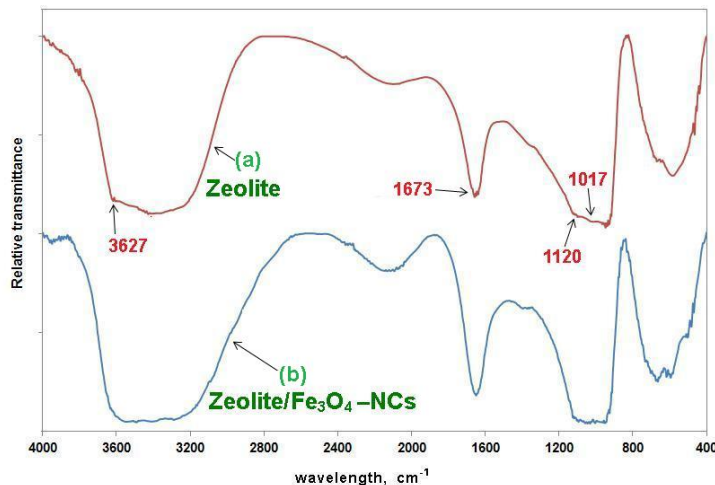


Fig. 2. The near FT-IR spectra of zeolite (a) and zeolite/Fe₃O₄-NCs (b)

3.2.2. Far FT-IR spectroscopy

The far FT-IR spectra of zeolite (A) and zeolite/Fe₃O₄-NCs (B) are shown Figure 3. The figure shows that the zeolite/Fe₃O₄-NCs spectra (B) significantly different from the zeolite spectra (A) in the spectral regions 300 to 700 cm⁻¹ due to the presence of Fe₃O₄-NPs in the zeolite. The peaks that appear in the zeolite/Fe₃O₄-NCs spectra (B) in the spectral regions 674 (a) and 661(b) cm⁻¹ [28], 585(c) cm⁻¹ [29, 30], 543 (d), 513(e), 493(f), 470(g) and 347(h) cm⁻¹ [28-30] correspond to Fe²⁺-O-Fe³⁺, Fe³⁺-O and Fe²⁺-O bonds from Fe₃O₄. Those peaks were not appeared in the zeolite spectra (A).

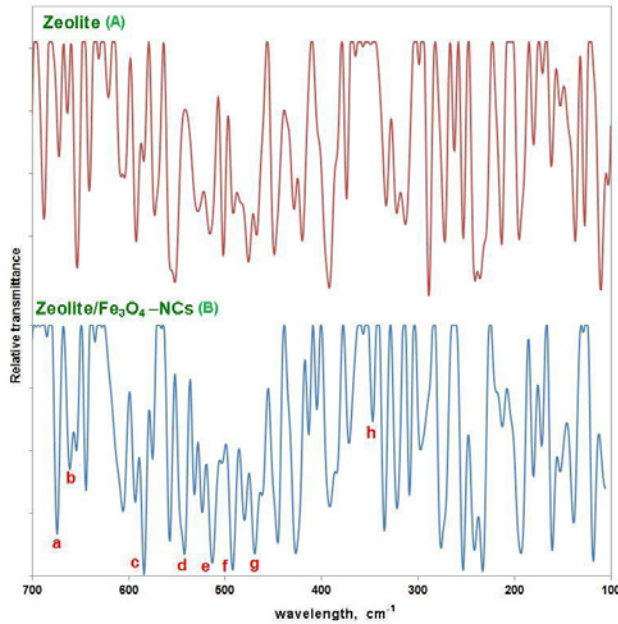


Fig. 3. The far FT-IR spectra of zeolite (A) and zeolite/Fe₃O₄-NCs (B)

3.3. Powder X-ray Diffraction (PXRD)

PXRD patterns of zeolite (A) and zeolite/Fe₃O₄-NCs (B) that were scanned in the small angle range of 2θ (15–25) are shown in the Figure 4. The figure shows that the pattern of zeolite peaks before (A) and after precipitation of Fe₃O₄-NCs (B) were similar showing that zeolite structure is stable and has not changed with the sum of reflection intensities peaks at 2θ of 30.92°, 32.66°, 34.16°, 35.5°, 35.82°, 36.6°, 38.18°, 40.28°, 41.66°, 42.98°, 43.64°, 44.26°, 47.44°, 47.96°, 49.82°, 52.26°, 54.36°, 56.56°, 57.68°, 58.74°, 65.32°, 66.82°, 71.14°, 73.04°. This is comparable to that of Treacy and Higgins at Collection of simulated XRD powder patterns for zeolites [31]. Also the zeolite/Fe₃O₄-NCs PXRD pattern (B) in Figure 4 shows four crystalline peaks at 2θ of 35.36°, 59.40°, 61.78° and 74.34° related to the (311), (511), (440) and (622) crystallographic planes of face-centered cubic (fcc) iron oxide nanocrystals, respectively (Ref. Code Fe3O4: 01-088-0315) [32,33]. These results confirmed that there are significant amount of Fe₃O₄-NPs were precipitated on the surface of zeolite as evidenced by the attraction of the powder particles of zeolite/Fe₃O₄-NCs to magnet.

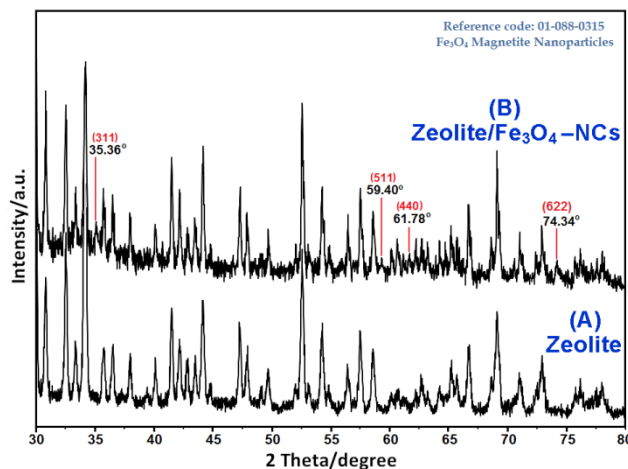


Fig. 4. PXRD patterns of zeolite (A) and zeolite/Fe₃O₄-NCs (B)

3.4. Scanning Electron Microscopy (SEM)

Fig. 5 shows the scanning electron microscopy (SEM) of zeolite (A, a) and zeolite/Fe₃O₄ – NCs (B, b). The figure shows that the shape of the particle are cubic structure showing that the zeolite structure has not changed by formation of Fe₃O₄ – NCs on the zeolite as shown by the results of FT-IR and XRD analyses. Also the comparison of SEM pictures of (A) and (B) in Figure 5 shows that in zeolite/Fe₃O₄ – NCs some particles aggregation has occurred due to synthesize of nanoparticles of Fe₃O₄ on the surface of zeolite. This can be clearly seen by comparing SEM pictures of Figure 5a and Figure 5b with high magnification which show that the Fe₃O₄-NPs have appeared as thin layer on surface of zeolite particles.

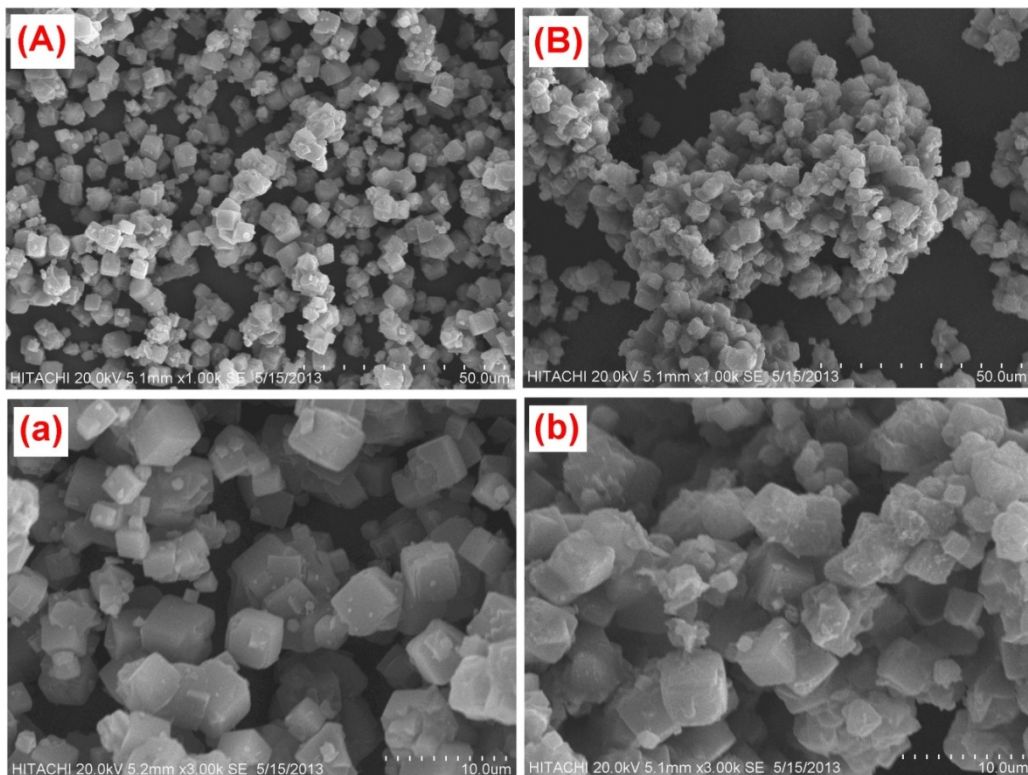


Fig. 5. SEM of zeolite (A), (a) and zeolite/Fe₃O₄ – NCs (B), (b)

3.5. Energy Dispersive X-ray Spectroscopy (EDX)

The elements present in zeolite (a) and zeolite/Fe₃O₄ – NCs (b) were analyzed by energy dispersive X-rays (EDX) and their results are shown in Figure 6. In the EDX spectra of zeolite Figure 6 (a), the appeared peaks in regions of 0.55, 1.05, 1.50 and 1.75 keV are related to the binding energies of O, Na, Al and Si, respectively which also have appeared in EDX spectra of zeolite/Fe₃O₄ – NCs Figure 6 (b). This confirms that the zeolite structure has not changed by synthesis of zeolite/Fe₃O₄ – NCs once again. Moreover in the EDX spectra of zeolite/Fe₃O₄ – NCs Figure 6 (b), the appeared peaks in regions of 6.4 and 7.05 keV are related to the binding energies of Fe which indicates the presence of iron in the product. Ma et. al. [34] and Chang et.al [35] reported similar EDX results for Fe₃O₄- NPs.

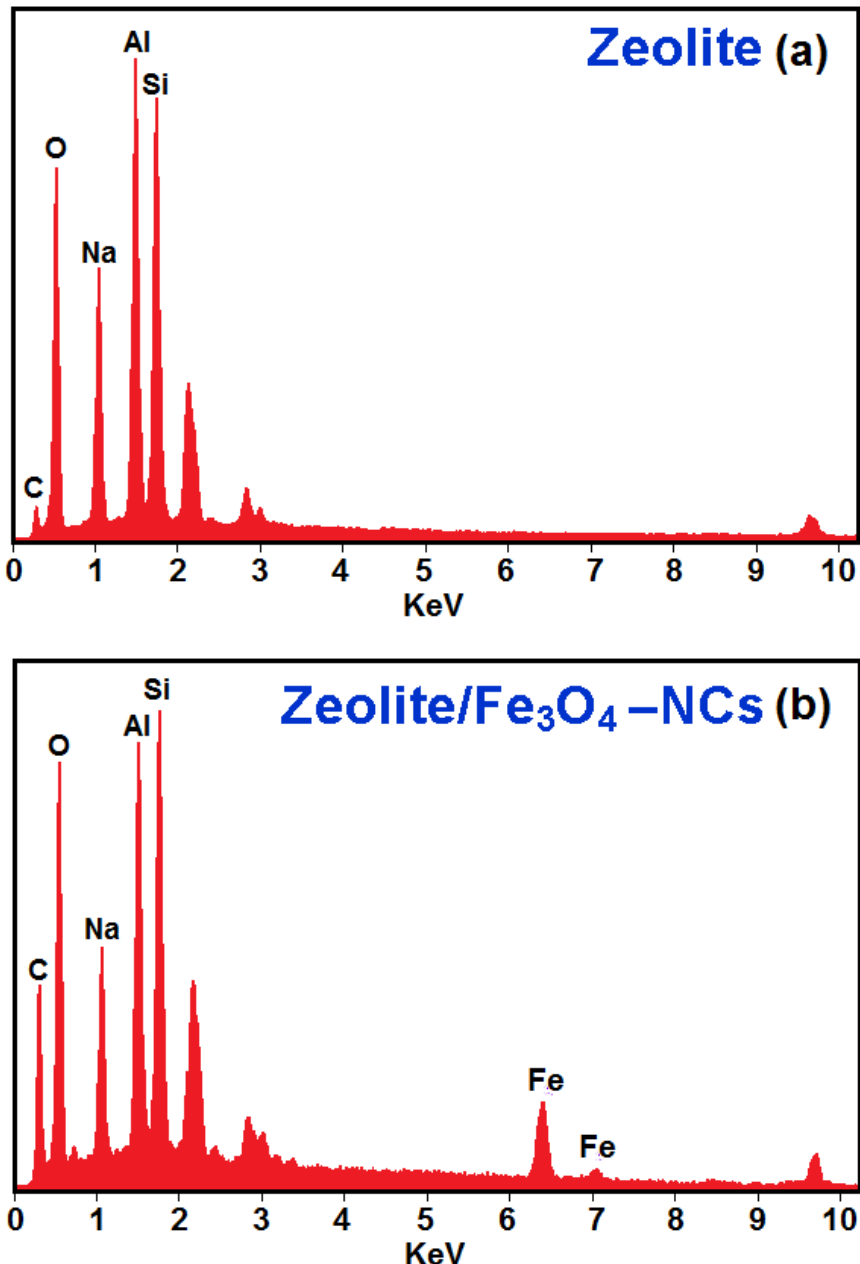


Fig. 6. EDX spectra of zeolite (a) and zeolite/Fe₃O₄-NCs (b)

3.6. Transmission Electron Microscopy (TEM)

The TEM image and histogram of particle sizes distribution of zeolite/Fe₃O₄-NCs are shown in Figure 7. The TEM image shows Fe₃O₄-NPs appear as spherical morphology with mean diameters of 3.55 ± 1.03 nm which is obtained from counting of 169 particles in the image. The result is better compared that reported by Ma et. al. who produced Fe₃O₄-NPs with average diameter of 7.5 nm when using FeCl₃ and FeSO₄ as iron sources and NH₄OH as precipitating agent [34].

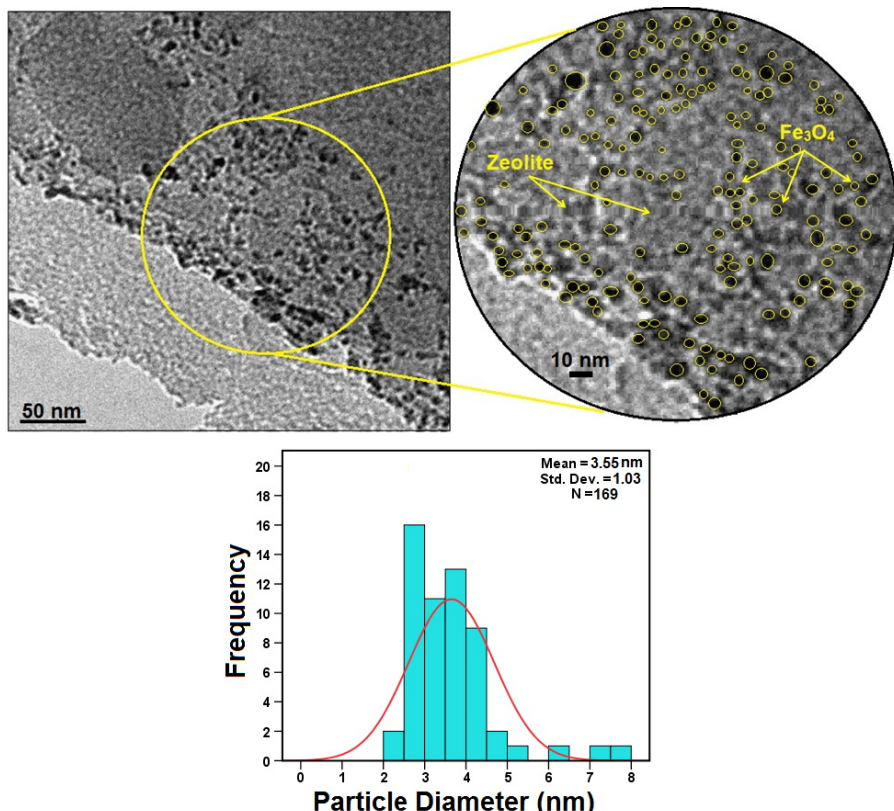


Fig. 7. TEM image and histogram of zeolite/Fe₃O₄-NCs

4. Conclusions

The zeolite/Fe₃O₄-NCs were synthesized from ferric chloride, ferrous chloride and sodium hydroxide aqueous solutions by quick precipitation on the surface of zeolite. The reaction was performed in aqueous suspension phase under the ambient conditions as one of its main advantages. Other advantages of this reaction are using friendly environmental and low cost raw materials. The mean particle sizes of Fe₃O₄-NPs in the product were 3.55 ± 1.02 nm. The obtained results of Fourier transforms infrared spectroscopy (FT-IR), powder X-ray diffraction (PXRD) analysis, scanning electron microscopy (SEM), energy dispersive X-ray fluorescence (EDXF) and transmission electron microscopy (TEM) confirmed the formation of zeolite/Fe₃O₄-NCs.

References

- [1] N. Gan, J. Zhou, P. Xiong, F. Hu, Y. Cao, T. Li, Q. Jiang, *Toxins*, **5** (5), 865 (2012).
- [2] J. Wu, H. Liu, Z. Lin, *Sensors*, **8**, (11), 7085 (2008).
- [3] X. Sun, Y. Cao, Z. Gong, X. Wang, Y. Zhang, J. Gao, *Sensors*, **12** (12), 17247 (2012).
- [4] C. Zet, C. Fosalau, *Dig. J. Nanomater. Bios.* **7** (1), 299 (2012).
- [5] M. Popescu, I. D. Simandan, F. Sava, A. Velea, E. Fagadar-Cosma, *Dig. J. Nanomater. Bios.*, **6** (3), 1253 (2011).
- [6] L. C. Battirola, L. H. S. Gasparotto, U. P. Rodrigues-Filho, G. Tremiliosi-Filho, *Membranes*, **2** (3), 430 (2012).
- [7] V. Melinte, T. Buruiana, I. D. Moraru, E. C. Buruiana *Dig. J. Nanomater. Bios.*, **6** (1), 213 (2011).
- [8] A. Sobczak-Kupiec, D. Malina, B. Tyliszczak, M. Piątkowski, K. Bialik-Wąs, Z. Wzorek *Digest Dig. J. Nanomater. Bios.*, **7**, (2), 459 (2012).
- [9] N. Rezlescu, E. Rezlescu, C. Doroftei, P.D. Popa, M. Ignat *Dig. J. Nanomater. Bios.*, **8** (2), 581 (2013).
- [10] L. Wang, X. He, C. A. Wilkie, *Materials*, **3** (9), 4580 (2010).
- [11] Z. Wang, A. Cuschieri, *Int J Mol Sci.*, **14** (5), 9111 (2013).

- [12] R. Khandanlou, M. Ahmad, K. Shameli, K. Kalantari, *Molecules*, **18** (6), 6597 (2013).
- [13] P. Granitzer, K. Rumpf, *Materials*, **4** (5), 908 (2011).
- [14] S.L. Iconaru, E. Andronescu, C.S. Ciobanu, A.M. Prodan, P. Le Coustumer, D. Predoi, *Dig. J. Nanomater. Bios.*, **7** (1), 399 (2012).
- [15] D. M. Nedeljković, A. P. Stajčić, A. S. Grujić, J. T. Stajić-Trošić, M. M. Zrilića, J. S Stevanović, S. Z. Drmanić, *Dig. J. Nanomater. Bios.*, **7** (1), 269 (2012).
- [16] H. M. Al-Matar, K. D. Khalil, M. F. Al-Kanderi, M. H. Elnagdi, *Molecules*, **17**(1), 897 (2012).
- [17] H. M. Ibrahim, H. Behbehani, S. Makhseed, M. H. Elnagdi, *Molecules*, **16** (5), 3723 (2011).
- [18] A. C. L. Batista, E. R. Villanueva, R. V. R. S. Amorim, M. T. Tavares, G. M. Campos-Takaki, *Molecules*, **16** (5), 3569 (2011).
- [19] K. Okumura, T. Tomiyama, S. Moriyama, A. Nakamichi, M. Niwa, *Molecules*, **16** (1), 38 (2010).
- [20] N. Pinna, S. Grancharov, P. Beato, P. Bonville, M. Antonietti, M. Niedereberger, *Chem. Mater.*, **17**, 3044 (2005).
- [21] W. S. Chiu, S. Radiman, M. H. Abdullah, P. S. Khiew, N. M. Huang, R. Abd-Shukor, *Mater. Chem. Phys.*, **106**, 231 (2007).
- [22] N. J. Tang, W. Zhong, X. L. Wu, H. Y. Jiang, W. Liu, Y. W. Du, *J. Magn. Magn. Mater.*, **282**, 92 (2004).
- [23] K. R. Vijaya, Y. Koltypin, Y. S. Cohen, Y. Cohen, D. Aurbach, O. Palchik, I. Felner, A. Gedanken, *J. Mater. Chem.*, **10**, 1125 (2000).
- [24] I. Martinez-Mera, M. E. Espinosa-Pesqueira, R. Pérez-Hernández, J. Arenas-Alatorre, *Mater. Lett.*, **61**, 4447 (2007).
- [25] C. Orha, A. Pop, C. Lazau, I. Grozescu, V. Tiponut, F. Manea, *J. Optoelectron Adv. Mater.*, **13** (5), 544 (2011).
- [26] E. M. Flanigen, H. Khatami, H. A. *Adv. Chem. Ser.*, **101**, 201 (1971).
- [27] A. Jentys, J.A. Lercher, *Studies in Surface Science and Catalysis* (Vol. **137**), Eds. H. van Bekkum, E.M. Flanigen, P.A. Jacobs, J.C. Jensen. Elsevier Science B.V., Amsterdam., 345 (2001).
- [28] Z. Guo, K. Lei, Y. Li, H. W. Ng, S. Prikhodko, H. T. Hahn, *Compos. Sci. Technol.*, **68** (6), 1513 (2008).
- [29] D. Predoi, *Dig. J. Nanomater. Biostruct.*, **2**, 169 (2007).
- [30] A. K. Gupta, S. Wells, *IEEE T. Nanobiosci.*, , **3** (1), 66 (2004).
- [31] M. M. J. Treacy, J. B. Higgins, Access Online via Elsevier: (2001).
- [32] L. Pislaru-Danescu, A. Morega, G. Telipan, *Optoelectron Adv. Mat.*, **8**, 1182 (2010).
- [33] P. Daraei, S. Madaeni, N. Ghaemi, E. Salehi, M. A. Khadivi, R. Moradian, B. Astinchap, *J. Membrane Sci.*, **415**, 250 (2012).
- [34] M. Ma, Y. Zhang, W. Yu, H.-y. Shen, H.-q. Zhang, N. Gu, *Colloids and Surfaces A: Physicochem. Eng. Aspects.*, **212**, 219 (2003).
- [35] Y. P. Chang, C. L. Ren, J. C. Qu, X. G. Chen, *Appl. Surf. Sci.*, **261**, 504 (2012)